HHS Public Access

Author manuscript

Conf Proc IEEE Eng Med Biol Soc. Author manuscript; available in PMC 2018 February 04.

Published in final edited form as:

Conf Proc IEEE Eng Med Biol Soc. 2015 August ; 2015: 679–682. doi:10.1109/EMBC.2015.7318453.

Creating Shape Templates for Patient Specific Biventricular Modeling in Congenital Heart Disease

Kathleen Gilbert,
Department of Anatomy, Faculty of Medical and Health Sciences, University of Auckland, New Zealand

Genevieve Farrar,
Department of Bioengineering, University of California San Diego, USA

Brett R. Cowan,
Department of Anatomy, Faculty of Medical and Health Sciences, University of Auckland, New Zealand

Avan Suinesiaputra,
Department of Anatomy, Faculty of Medical and Health Sciences, University of Auckland, New Zealand

Christopher Occleshaw,
Department of Anatomy, Faculty of Medical and Health Sciences, University of Auckland, New Zealand

Beau Pontré,
Department of Anatomy, Faculty of Medical and Health Sciences, University of Auckland, New Zealand

James Perry,
Department of Pediatrics, University of California San Diego, USA

Sanjeet Hegde,
Department of Pediatrics, University of California San Diego, USA

Alison Marsden,
Department of Mechanical and Aerospace Engineering, University of California, San Diego, USA

Jeff Omens,
Department of Bioengineering, University of California San Diego, USA

Andrew McCulloch, and
Department of Bioengineering, University of California San Diego, USA

Alistair A. Young
Department of Anatomy, Faculty of Medical and Health Sciences, University of Auckland, New Zealand

Abstract

Survival rates for infants with congenital heart disease (CHD) are improving, resulting in a growing population of adults with CHD. However, the analysis of left and right ventricular

function is very time-consuming owing to the variety of congenital morphologies. Efficient customization of patient geometry and function depends on high quality shape templates specifically designed for the application. In this paper, we combine a method for creating finite element shape templates with an interactive template customization to patient MRI examinations. This enables different templates to be chosen depending on patient morphology. To demonstrate this pipeline, a new biventricular template with 162 elements was created and tested in place of an existing 82-element template. The method was able to provide fast interactive biventricular analysis with 0.31 sec per edit response time. The new template was customized to 13 CHD patients with similar biventricular topology, showing improved performance over the previous template and good agreement with clinical indices.

I. INTRODUCTION

Approximately 75 in 1000 infants are born with congenital heart disease (CHD) each year [1]. Those with severe disease are living longer due to better interventions in early life, resulting in a growing population of adult CHD patients [2]. Patients with CHD require regular imaging in order to monitor their cardiac function. Many of these lesions have an impact on the right ventricle [3].

Magnetic resonance imaging (MRI) with manual contouring is considered the gold standard for assessing cardiac function, and has been increasingly referred for pediatric patients with CHD particularly when clinical or echocardiographic examination is insufficient for decision making on a surgical treatment [4]. MRI does not use ionizing radiation, has good resolution and is non-invasive. Manual analysis of both the left (LV) and right ventricle (RV), to obtain the mass and volumes, is however still time-consuming [5]. While some semi-automated [6] methods are available for biventricular segmentation, these are typically not suitable for assessing patients with CHD, due to the large variation in pathology. Specific segmentation algorithms have been developed for RV segmentation, however most previous methods ignore the position and motion of the valves [7] which are a major source of error in mass and volume. Previously, biventricular modeling methods have been developed that use subdivision surfaces [8] and 4D spatio-temporal models [9]. Lamata et al. [10] proposed a customization method for biventricular modelling; however, it did not include any valves and only produced a model for one timepoint in the cardiac cycle.

We developed a method for interactive customization of biventricular geometry and function in CHD [11]. Briefly, the method deforms a finite element model template to fit the MR images of patients with CHD throughout the entire cardiac cycle. Polar prediction and D-Affine regularization were shown to improve the customization process. D-Affine regularization minimizes variation in deformation of the template during the customization process, and is invariant to affine transformations. However, there are a wide variety of congenital heart disease manifestations (Fig. 1). In many cases significant morphological changes are required in order to accurately assess shape and function, due to the variety of right and left ventricle shapes. It would be advantageous to have multiple templates that represent different pathologies. These should be able to model a variety of lesions including single ventricle pathologies. Consequently, the mesh topology and number of elements could

vary from case to case. The trade-off for this complexity would be faster analysis time and more accurate customization to a wide variety of pathologies. The current template was developed from a porcine model, and contains collapsed and hanging nodes [12]. The template was time consuming to create and it would not be feasible to create multiple templates using this methodology. Recently, Gonzales et al. [13] presented a flexible method to define a finite element model (FEM) topology using extraordinary nodes. This method can quickly create an arbitrary topology using a combination of image analysis and computer graphics. In this paper, we extended the interactive biventricular guide-point modeling method presented in [11] to enable templates created using [13] of arbitrary topology to be inputed and customized using rapid D-Affine shape customization. We demonstrate this pipeline using a biventricular template created from CT, showing improved performance during customization to dynamic MRI data, and assess resulting clinical indices in 13 CHD patients against traditional manual contouring methods.

II. METHODS

A. Template

The method presented in [13] was used to create a biventricular finite element template of arbitrary topology. Briefly, a bilinear mesh topology was interactively defined using *Blender* (www.blender.org) by placing nodes on the epicardial and endocardial surfaces of a segmented 3D image dataset (Fig. 2 top row). The bilinear topology was then subdivided using a Li-Kobbelt subdivision scheme [14], in order to provide an approximately C^1 surface. The subdivided points (Fig. 2 bottom row) were used to generate a tricubic Hermite finite element mesh [13].

B. General Linear Map

We adopted the general linear map proposed by Nielsen [15] to describe finite element models of arbitrary topology and continuity. Global mesh parameters were defined as those mesh degrees of freedom which are directly modifiable by the patient specific customization process. Eight global parameters were chosen per node, defining the node position and derivatives with respect to element coordinates (s_1, s_2, s_3) for one of the elements adjoining the node. Given an adjoining element with element coordinates (t_1, t_2, t_3), a mapping between element coordinates could be defined as

$$t = Js \quad (1)$$

where J is the Jacobian matrix $\frac{\partial t_i}{\partial s_j}$. Derivatives with respect to t could then be calculated as:

$$\frac{\partial Y}{\partial t_i} = \sum \frac{\partial Y}{\partial s_k} \frac{\partial s_k}{\partial t_i}, i, k \in 1, 2, 3 \quad (2)$$

The cross derivatives can be calculated in a similar fashion. Derivative continuity between elements could then be maintained by these linear constraints between global (with respect

to s) parameters and local (with respect to t) parameters adjoining each node. Local parameters (p) were then defined to be a linear combination of global parameters (P):

$$p=GP \quad (3)$$

where G is a sparse $M \times N$ matrix for M local and N global parameters. Swapping templates then simply involves reading another general linear map, which may have different dimensions.

C. Parameter Reduction and Customization—Since non-linear transmural deformation was not required for our application, we reduced the interpolation in the transmural direction from cubic to linear. Also, for our application, it was desirable to have all shape parameters in the same units. We therefore converted the Hermite parameters to Bézier parameters using the standard linear mapping [16]. This produced a bicubic Bézier template, which was customized to particular patient images using D-Affine warping with polar prediction [11].

Briefly, the guide-point modeling method, described in Gilbert et al. [11] involves the template being customized by warping the geometry to fit the location of guide points interactively placed by the user on cine MR image datasets. Points were first placed on the valve annuli and the left ventricular apex in the long axis images, followed by additional points placed on the inner (endocardial) and outer (epicardial) surfaces of the heart as necessary. Each edited model contour, as well as all valve and apex points, were automatically tracked through the cardiac cycle using non-rigid registration [17] and the resulting tracked contour points were included in the model fit at each frame. At each iteration, a prolate spheroidal geometry was fitted to the epicardium and LV endocardial surface, followed by a biventricular Cartesian model fit to the polar surfaces with a high regularization parameter. User-defined guide points and tracked contour points were then projected onto the closest biventricular model point and the fit updated using a low regularization parameter. After each interaction, tracked contour points were regenerated for all frames. The regularization term penalized the deviation of the warp from affine deformations.

III. Results

A CT 3D dataset (General Electric 64-slice Lightspeed CT Scanner, 0.5 × 0.5 × 0.625 mm voxel size, retrospective gating) was obtained from a patient with atrial fibrillation, with local IRB approval and written informed consent. This dataset was chosen to be approximately normal that could be fitted to a wide range of shapes. A bilinear topology was defined interactively using Blender [13]. This topology, shown in fig. 2 (top row), had 162 elements and 338 nodes, of which 24 were extraordinary (i.e. valence 5 or 3). Each element was subdivided twice using the Li-Kobbelt scheme, and the resulting points were used to define a tricubic Hermite model. This mesh was exported from Blender as a list of 64 tricubic Hermite parameters per hexahedral element, resulting in $M = 64 \times 162 = 10368$ element (local) parameters per x,y,z coordinate [13]. Each node was assigned 8 global

parameters giving N=2704 global parameters in total. After conversion to bicubic Bézier basis functions with linear transmural interpolation, the resulting template had 1352 global parameters. The MRI images used for this study were acquired using short and long axis retrospectively gated SSFP MRI cine images (Siemens 1.5T scanner, 30ms repetition time, 1.6ms echo time, 60° flip angle, 360 × 360mm field of view, 6mm slice thickness, 256×208 image matrix. Ethical approval was granted from the institutional ethics committee, with written informed consent from all patients.

A. Screen Updating and Solver

The template was customized to MR images of a patient with surgically corrected dextro-transposition of the great arteries (fig. 3). The same case was assessed using both the original 82-element model and the new 162-element model on a Dell OptiPlex 990 with an Intel(R) Core i5 3.30GHz with 4GB of RAM and running Windows 7.

The preconditioned conjugate gradient method (PCG), with multi-threading, was tested with two tolerance levels: 1×10^{-9} with a maximum of 200 iterations and 1×10^{-4} with a maximum of 100 iterations. Table 1 shows the results (some cases did not fully converge for the 82-element model, leading to a higher residual than the tolerance on average). The method is interactive, therefore the updating must be almost real-time. The time taken for the model to incorporate a change into the data structures and update the contour on the screen (known as drag time) was collected. The drag times were 0.31s and 0.19s for the new and original model respectively. The new template showed faster convergence than the 82-element model, possibly because the latter employed collapsed element edges at the apex, whereas the former used extraordinary nodes to avoid collapsing elements.

B. Clinical Outcomes

The new template was then fitted to 13 patients with CHD where gold standard manual contours were available. The manual contours were drawn using Argus (Syngo MR 2004V, Siemens Medical Solutions, Erlangen, Germany). The new template took between 1200 and 2520 seconds (average 1779.6 seconds) to fit each case, compared with 1966.8 seconds with the previous template [11]. The end-diastolic volume (EDV), end-systolic volume (ESV), mass and ejection fraction (EF) of both ventricles were recorded. Fig. 4 shows a comparison of the clinical measures of heart function between the biventricular modeler and manual contours. Table 2 shows the average value and differences and standard deviation of differences.

IV. Discussion and Conclusions

We have presented a novel pipeline for evaluating spatiotemporal biventricular function, resulting in a flexible tool for modeling the complex pathologies seen in patients with CHD.

While analysis of mass and volumes is important in a clinical setting, well-designed anatomical modeling techniques can also provide valuable shape information and be suitable for simulating physiological functions such as electrophysiology and biomechanics. The rapid biventricular modeler can be ported directly into finite element solvers, such as

Continuity (fig. 5). The pipeline to create customizable templates was automated, so that new templates can be created and customized as required.

The new template produced good correlation of mass and volume. The bias between the biventricular tool and manual analysis is due to differences in identification of ventricular blood and mass below the four valves, which is a known source of error in contouring short axis slices [5]. The model uses 3D locations of the valves and is expected to be more accurate. The precision (variance of differences) were clinically acceptable compared with the enlarged volumes seen in these patients.

Although the new template has more than twice the number parameters of the original model, the preconditioned conjugate gradient method was able to solve with significantly fewer iterations, resulting in a smaller increase in the drag time than expected (Table 1). Further work is necessary to determine what tolerance is required for clinical use. At present, 1×10^{-4} is used for interactive dragging, and 1×10^{-9} is used for the final update.

The analysis time suggests that while this template was easily customised to some cases, it would be advantageous to create several templates, with a range of shapes and allow the user to pick the one that is closest to the anatomy that is being analysed. This would reduce the amount of customisation required and therefore total time required for analysis.

Acknowledgments

This work was supported by NHLBI R01 HL121754. Kathleen Gilbert is supported by an award from the Green Lane Research and Educational Fund Board. The Authors also gratefully acknowledge support from the National Heart foundation of New Zealand.

References

1. Fogel, MA. Ventricular Function and Blood Flow in Congenital Heart Disease. John Wiley & Sons; 2005.
2. Bricker ME, Hills LD, Lange RA. Congenital Heart Disease in Adults First of Two Parts First. The New Journal of Medicine. 2000; 342:256–263.
3. Haddad F, Doyle R, Murphy DJ, Hunt SA. Right ventricular function in cardiovascular disease, part II: pathophysiology, clinical importance, and management of right ventricular failure. Circulation. Apr; 2008 117(13):1717–31. [PubMed: 18378625]
4. Ntsinjana HN, Hughes ML, Taylor AM. The role of cardiovascular magnetic resonance in pediatric congenital heart disease. Journal of cardiovascular magnetic resonance: official journal of the Society for Cardiovascular Magnetic Resonance. Jan.2011 13(1):51. [PubMed: 21936913]
5. Hudsmith L, Petersen S, Francis J, Robson M, Neubauer S. Normal Human Left and Right Ventricular and Left Atrial Dimensions Using Steady State Free Precession Magnetic Resonance Imaging. Journal of Cardiovascular Magnetic Resonance. Oct; 2005 7(5):775–782. [PubMed: 16353438]
6. Wang Z, Salah MB, Gu B, Islam A, Goela A, Li S. Direct estimation of cardiac biventricular volumes with an adapted Bayesian formulation. IEEE transactions on bio-medical engineering. Apr; 2014 61(4):1251–60. [PubMed: 24658249]
7. Petitjean, Caroline. RV Segmentation Challenge in Cardiac MRI. [Online]. Available: http://www.litislab.eu/rvsc/workshop/rv-segmentation-challenge-in-cardiac-mri
8. Hubka M, Bolson EL, McDonald Ja, Martin RW, Munt B, Sheehan FH. Three-dimensional echocardiographic measurement of left and right ventricular mass and volume: in vitro validation. The international journal of cardiovascular imaging. Apr; 2002 18(2):111–8. [PubMed: 12108906]

9. Perperidis D, Mohiaddin RH, Rueckert D. Spatio-temporal free-form registration of cardiac mr image sequences. Medical image analysis. 2005; 9(5):441–456. [PubMed: 16029955]
10. Lamata P, Niederer S, Nordsletten D, Barber DC, Roy I, Hose DR, Smith N. An accurate, fast and robust method to generate patient-specific cubic hermite meshes. Medical image analysis. 2011; 15(6):801–813. [PubMed: 21788150]
11. Gilbert, K., Cowan, BR., Suinesiaputra, A., Occleshaw, C., Young, AA. Medical Image Computing and Computer Assisted Intervention MICCAI. Springer International Publishing; 2014. Rapid D-Affine Biventricular Cardiac Function with Polar Prediction; p. 546-553.
12. Lam, H-I., Cowan, BR., Nash, MP., Young, AA. Statistical Atlases and Computational Models of the Heart. Springer; 2010. Interactive cardiac image analysis for biventricular function of the human heart; p. 144-153.
13. Gonzales MJ, Sturgeon G, Krishnamurthy A, Hake J, Jonas R, Stark P, Rappel WJ, Narayan SM, Zhang Y, Segars WP, McCulloch AD. A three-dimensional finite element model of human atrial anatomy: new methods for cubic Hermite meshes with extraordinary vertices. Medical image analysis. Jul; 2013 17(5):525–37. [PubMed: 23602918]
14. Li G, Ma W, Bao H. A New Interpolatory Subdivision for Quadrilateral Meshes. Computer Graphics Forum. Mar; 2005 24(1):3–16.
15. Nielsen, PMF. PhD thesis. Unviersity of Auckland; 1987. The Anatomy of the Heart: A Finite Element Model.
16. Foley, JD., Van Dam, A., Feiner, SK., Hughes, JF., Phillips, RL. Introduction to computer graphics. Addison-Wesley Reading; 1994.
17. Li B, Liu Y, Occleshaw CJ, Cowan BR, Young AA. In-line automated tracking for ventricular function with magnetic resonance imaging. JACC Cardiovascular imaging. Aug; 2010 3(8):860–6. [PubMed: 20705268]

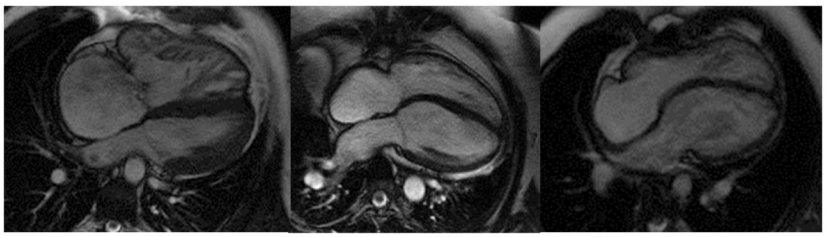

Fig. 1.

Long-axis MR images of three patients with CHD. The image on the left is from a patient with pulmonary atresia and the following two are patients with Tetralogy of Fallot.

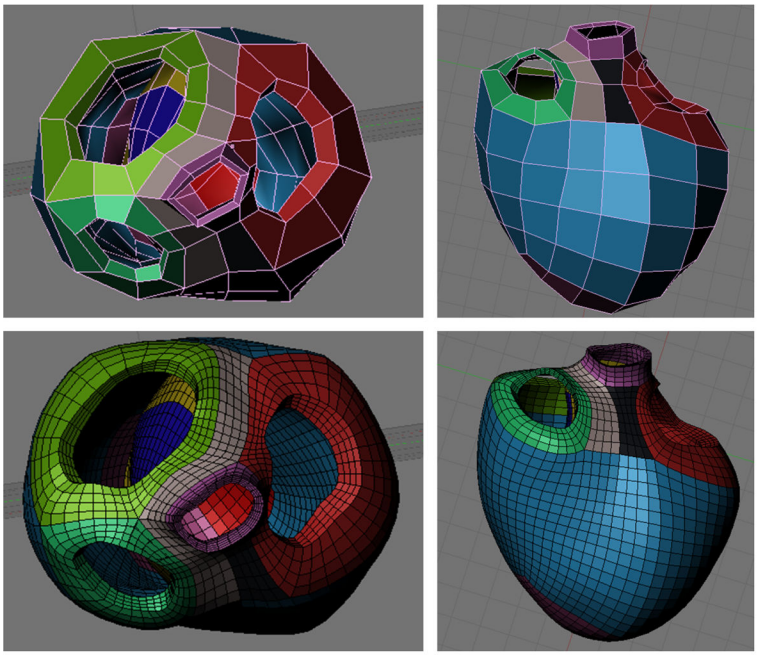

Fig. 2.

The tricubic mesh exported from Blender. The top two images show the actual element size. The bottom two images show the mesh after a Li-Kobbelt subdivision. C1 continuity was maintained exactly within the colored topology regions and approximately between regions.

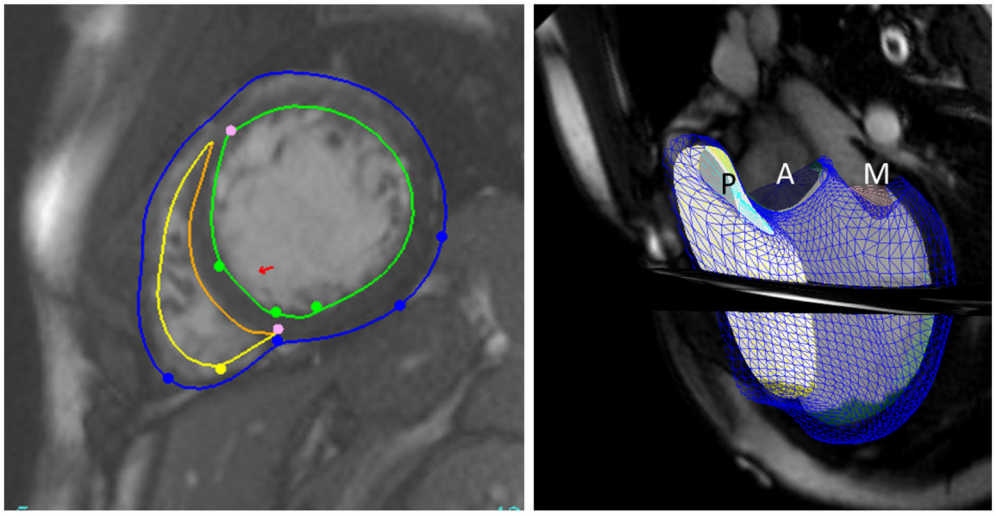

Fig. 3.

Customization of the new template to a patient with surgically corrected dextro-transposition of the great arteries using guide point modeling. The image on the left is a 2D contour customization and the image on the right is the customized model in 3D. The red arrow on the 2D contour shows in plane shifting to account for breath hold mis-registration. The mitral valve is labeled by M, the aortic valve by A, and the pulmonary by P on the 3D image.

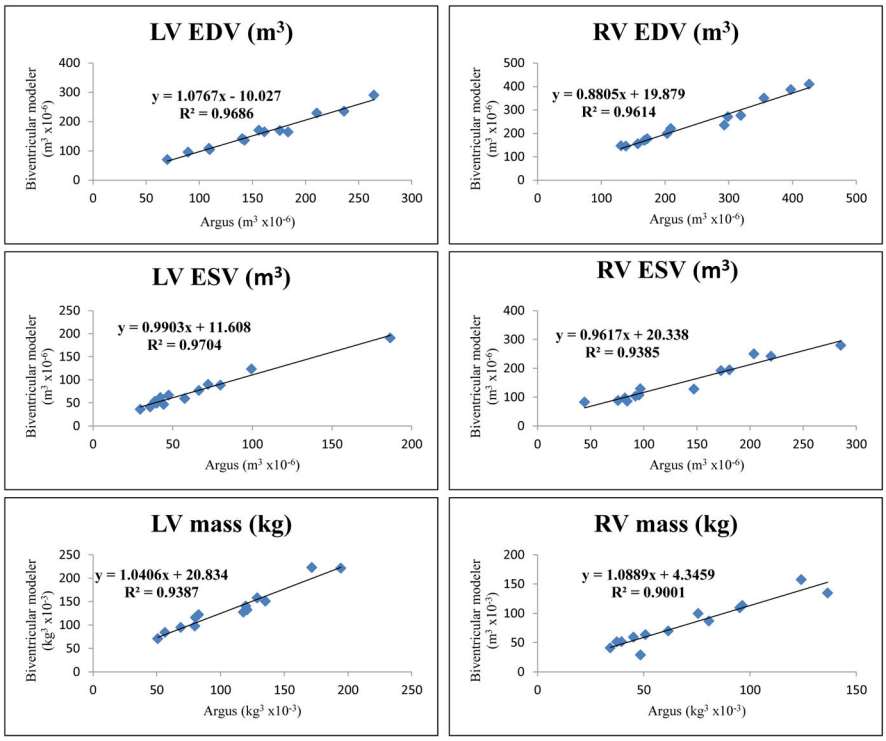

Fig. 4.

Comparison of Clinical measures of heart function (LV EDV, RV EDV, LV ESV, RV ESV, LV mass and RV mass) between the biventricular modeler and gold standard Argus contours.

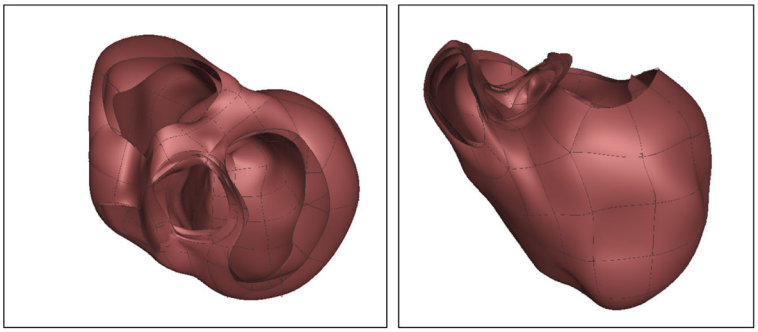

Fig. 5.

Customized cubic Hermite model of the same patient with surgically corrected dextro-transposition of the great arteries as Figure 3. loaded into Continuity (http://www.continuity.ucsd.edu/) for further analysis of stress and activation.

TABLE I

Average convergence time

	Original 82-Element model		**New 162-Element model**	
Tolerance	1×10^{-4}	1×10^{-9}	$1.\times10^{-4}$	1×10^{-9}
Solution time (s)	0.016	0.033	0.017	0.071
Number of iterations	91.8	199.4	10.9	41.7
Average residual error	0.002	0.0001	$<1\times10^{-4}$	$<1\times10^{-9}$

TABLE II

Average values and difference between two methods with one standard deviation.

	LV EDV	RV EDV	LV ESV	RV ESV	LV mass	RV mass	LV EF	RV EF
	$m^3 \times 10^{-6}$				$kg \times 10^{-3}$		%	
Average Value	158.8±55.0	246.5±89.1	70.2±38.7	144.6±64.8	120.9±41.5	76.6±33.04	57.0±9.3	42.8±7.3
Average Difference	−2.1±11.9	10.2±21.7	−11.0±7.2	−15.1±17.6	−25.2±11.7	−10.7±12.6	6.6±5.5	8.9±6.6

Conf Proc IEEE Eng Med Biol Soc. Author manuscript; available in PMC 2018 February 04.